Chemistry–A European Journal
Research Article
doi.org/10.1002/chem.202202648
Chemistry Europe
European Chemical Societies Publishing
www.chemeurj.org

Highly Cytotoxic Molybdenocenes with Strong Metabolic Effects Inhibit Tumour Growth in Mice

Valentin Fuchs,[a, d] Klaudia Cseh,[a] Michaela Hejl,[a] Petra Vician,[b, d] Benjamin Neuditschko,[a, c] Samuel M. Meier-Menches,[a, c, e] Lukas Janker,[c, e] Andrea Bileck,[c, e] Natalie Gajic,[a] Julia Kronberger,[a] Martin Schaier,[c] Sophie Neumayer,[c] Gunda Köllensperger,[c] Christopher Gerner,[c, e] Walter Berger,[b, d] Michael A. Jakupec,[a, d] Michael S. Malarek,*[a, d] and Bernhard K. Keppler[a, d]

Abstract: A series of six highly lipophilic Cp-substituted molybdenocenes bearing different bioactive chelating ligands was synthesized and characterized by NMR spectroscopy, mass spectrometry and X-ray crystallography. In vitro experiments showed a greatly increased cytotoxic potency when compared to the non-Cp-substituted counterparts. In vivo experiments performed with the dichlorido precursor, $(Ph_2C–Cp)_2MoCl_2$ and the in vitro most active complex, containing the thioflavone ligand, showed an inhibition of tumour growth. Proteomic studies on the same two compounds demonstrated a significant regulation of tubulin-associated and mitochondrial inner membrane proteins for both compounds and a strong metabolic effect of the thioflavone containing complex.

Introduction

Due to the debilitating side effects and resistance problems of classic platinum-based cancer treatments, the search for better drugs has expanded to other metals. Since molybdenum is the only second-row transition element necessary for life, present in multiple enzymes in the human body, we see great potential, with the correct choice of ligands, for a more tolerable drug.

The anti-cancer activity of titanium, vanadium, tungsten and molybdenum metallocenes (Cp_2MCl_2 ($Cp = \eta^5$-C_5H_5 and M=Ti, V, W, Mo) was first reported in 1979 by Köpf-Maier and Köpf, who tested the dichlorido complexes against Ehrlich ascites tumours in mice.[1–4] Cp_2TiCl_2 was found to be the most active in colon, breast and lung cancers and was studied in clinical trials, but was dismissed after phase II due to problems caused by dose-limiting toxicity and relatively low activity.[5–8] Recently, Titanocene Y (Figure 1), a Cp-substituted analogue of titanocene dichloride, has shown promising results in preclinical stages.[9]

Molybdenocene dichloride was found to be active in vivo against a number of cancers[3] and exhibits better hydrolytic stability than titanocene dichloride. At physiological pH, hydrolysis of the chlorido ligands leads to the formation of a (μ-

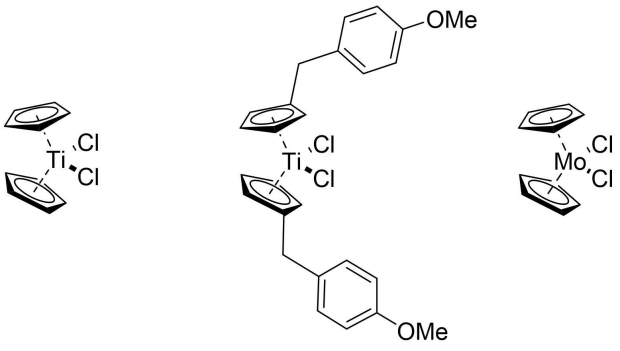

Figure 1. Structures of titanocene dichloride, Titanocene Y and molybdenocene dichloride (left to right).

[a] V. Fuchs, K. Cseh, M. Hejl, B. Neuditschko, Prof. Dr. S. M. Meier-Menches, N. Gajic, J. Kronberger, Dr. M. A. Jakupec, M. S. Malarek, Prof. Dr. B. K. Keppler
Institute of Inorganic Chemistry
University of Vienna
Währinger Straße 42, 1090 Vienna (Austria)
E-mail: michael.malarek@univie.ac.at

[b] P. Vician, Prof. Dr. W. Berger
Center for Cancer Research
Medical University of Vienna
Borschkegasse 8 A, 1090 Vienna (Austria)

[c] B. Neuditschko, Prof. Dr. S. M. Meier-Menches, L. Janker, A. Bileck, M. Schaier, S. Neumayer, Prof. Dr. G. Köllensperger, Prof. Dr. C. Gerner
Institute of Analytical Chemistry
University of Vienna
Währinger Straße 38, 1090 Vienna (Austria)

[d] V. Fuchs, P. Vician, Prof. Dr. W. Berger, Dr. M. A. Jakupec, M. S. Malarek, Prof. Dr. B. K. Keppler
Research Cluster "Translational Cancer Therapy Research"
Währinger Straße 42, 1090 Vienna (Austria)

[e] Prof. Dr. S. M. Meier-Menches, L. Janker, A. Bileck, Prof. Dr. C. Gerner
Joint Metabolome Facility
University of Vienna and Medical University of Vienna
Währinger Straße 38, 1090 Vienna (Austria)

Supporting information for this article is available on the WWW under https://doi.org/10.1002/chem.202202648

$OH)_2$ dimeric species, maintaining the Mo–Cp bond in contrast to titanocene dichloride.[10]

Vera et al. investigated the interactions of molybdenocene dichloride with nucleobases and phosphoesters and found weak binding,[11] while studies of Harding et al. suggest thiol interactions to be crucial for the anti-cancer activity of molybdenocene dichloride.[12] This is also supported by studies involving molybdenocene derivatives where the labile chlorido ligands had been replaced with thiols; these complexes, while exhibiting good cellular uptake, had significantly decreased cytotoxic activity.[13] Molybdenocene dichloride has been found to inhibit protein kinase C (PKC) and human topoisomerase II (Topo II), both of which play an important role in DNA replication and cell proliferation.[14,15]

Molybdenocene derivatives where the chlorido ligands had been replaced with chelating maltolato or malonato ligands showed slightly improved activity in HT-29 colon cancer cells compared to Cp_2MoCl_2, while exhibiting proliferative activity in hormone-dependent MCF-7 breast cancer cells.[16] Molybdenocenes bearing (S,N)-chelating thionucleobases and thionucleosides show decreased cytotoxic activity compared to the free ligands in colon cancer cell lines but enhanced cytotoxicity in breast cancer cell lines.[17]

Previously, our group reported six molybdenocenes bearing (N,O)-, (O,O)- and (O,S)- coordinating, bioactive, bidentate ligand scaffolds. Some of these were significantly cytotoxic.[18]

In this work, a novel molybdenocene bearing highly lipophilic diphenylmethyl substituents on both cyclopentadienyl rings was synthesised and the chlorido ligands were substituted for the same bioactive chelates used in previous works[18] in order to enable a direct comparison with the parent compounds. This facilitated an evaluation of the impact of the increased lipophilicity on the anticancer activity of these compounds. The chosen ligands were maltol, a non-toxic pyrone, which has been extensively studied as a chelator for a wide variety of metals,[19] as well as its highly cytotoxic, thionated analogue, thiomaltol, with IC_{50} values in the low- to submicromolar range in different human cancer cell lines.[20] In addition, phthiocol, a member of the naphthoquinone substance class, which exhibits a broad spectrum of potential anticancer activities,[21] picolinic acid, which showed antitumor activity in mice,[22] and a thionated flavone analogue, all of which show diverse pharmacological properties including anticancer, anti-inflammatory and antioxidant activities,[23] were employed as bidentate ligands.

Results and Discussion

Chemistry

The synthesis of compound **1** from 6,6′-diphenylfulvene (Scheme 1) constitutes a slight variation of the synthesis published for molybdenocene-analogues of Titanocene Y.[24] It could stand to be improved, however; we found that isolating the lithium cyclopentadienide and $MoCl_4$*$2Et_2O$ had no effect on the yield, when compared to generating them in situ, from the fulvene and super hydride, and $MoCl_5$ and granular tin, respectively, as outlined for the one-pot synthesis described here. Replacement of the chlorido ligands with the same bioactive chelates as previously described for molybdenocene dichloride was carried out according to Scheme 1. We found that the use of a mixture of dichloromethane (DCM) and MeOH allowed for shorter reaction times than described for the synthesis of the parent compounds where MeOH was used as the sole solvent.[18]

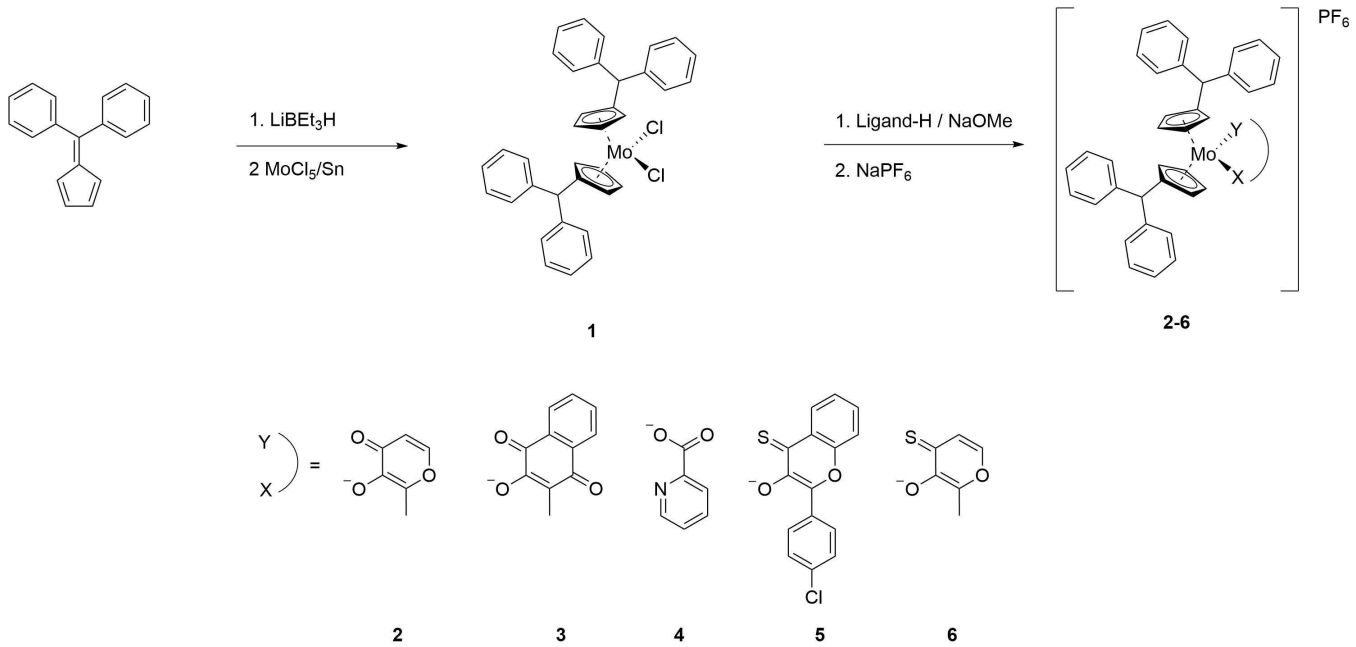

Scheme 1. General synthetic route for compounds **1**–**6**.

Unsurprisingly, the increase in lipophilicity led to decreased water solubility, and for most compounds of this series the solubility in 1% DMSO/water was insufficient for biological evaluation. Therefore, polyvinylpyrrolidone (PVP, avg. molecular weight 10,000 g/mol), a non-toxic, water soluble polymer which was initially used as a plasma expander and nowadays is used in a wide variety of medical applications, was chosen as a solubilizer.[25,26] The compounds were mixed with 10 times the amount (w/w%) of PVP, dissolved in DCM and dried in vacuo to afford a water-soluble solid mixture. This approach allowed the dissolution of the compounds in sufficient concentrations (> 1 mg/mL) for biological tests.

Stability by UV/Vis

The stability of these mixtures in aqueous media (phosphate buffered saline, pH = 7.4) was determined by UV/Vis Spectroscopy over the course of 24 h at 25 °C (see Supporting Information Figures S8-S13). Compounds **1** and **3** appear to degrade in solution (30% and 15% degradation over 6 h, respectively) with the latter exhibiting an isosbestic point at ~410 nm, indicating two species to exist in equilibrium, while the rest of the compounds show no change in their absorption patterns over this timespan; the remaining compounds precipitated to various degrees over time – mostly so compound **4** with about two thirds of the compound precipitated over the first 6 h.

X-ray diffraction analyses

Single crystals of the compounds were obtained by slow diffusion of *n*-hexane into an EtOAc solution (compound **1**) or Et_2O into DCM solutions (compounds **2**–**6**). Structures of **1** and **5** are shown in Figure 2. Experimental data, CCDC-codes, crystal data, data collection parameters and structure refinement information as well as visualizations of all asymmetric units can be found in the Supporting Information (Figures S26-S31).

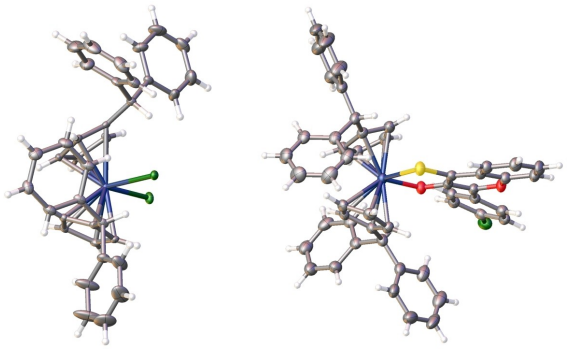

Figure 2. Molecular structures of compounds **1** (left) and **5** (right) with 50% displacement ellipsoids. Solvent molecules and counter ion are omitted for clarity.

Electrochemistry

The electrochemical behavior of compound **1** was determined by cyclic voltammetry (Figure S7). Comparison of the cyclic voltammogram to previously published data for molybdenocene dichloride[18,27] shows that both the reversible Mo(IV)↔Mo(V) oxidation and the irreversible Mo(IV)→Mo(II) reduction are shifted to a more positive potential. A third process is observed at 0.4 V, however, this process only occurs after scanning into negative potential, and in fact no processes were observed scanning only the physiological region [−0.320 V ($NADP^+ + H^+ + 2e^- \rightarrow NADPH$) to +0.820 V ($O_2 + 4H^+ + 4e^- \rightarrow 2H_2O$)].

Cytotoxicity in cancer cell lines

Results of MTT assays reveal that the chelated derivatives **2**–**6** show increased cytotoxic potency compared to the parent dichlorido complex **1** in all three tested human cancer cell lines (ovarian teratocarcinoma CH1-PA1, colon cancer SW480, lung cancer A549), but they suggest a dichotomy with regard to the degree of this increase (Table 1, Figure S20). While the phthiocol (**3**) and picolinate (**4**) analogues are moderately more potent than **1** (from an almost negligible 1.4 times to a maximum of 5.7 times, depending on the compound and cell line), the maltol (**2**), thioflavone (**5**) and thiomaltol (**6**) analogues are by more than an order of magnitude more potent throughout (from almost 50 times in the case of **2** to about 400 times in the case of **5**, each in A549 and SW480 cells). While the IC_{50} values of **1**, **3** and **4** are mostly still in the two-digit micromolar range, nearly all of **2**, **5** and **6** are sub-micromolar. There are clear structure-activity relationships for the ligand dependency of cytotoxicity, applicable to all three cell lines: thioflavone > thiomaltol > maltol ≫ phthiocol/picolinate > dichlorido.

In comparison with previous work from our group, on the non-Cp substituted counterparts[18] (**P1**–**P6**, Table 1), all new compounds show a marked increase in cytotoxicity. Interestingly, even the coordination motifs that showed no activity for the unsubstituted molybdenocene (dichlorido, maltolato and picolinato) (**P1**, **P2** and **P4**) show moderate (**1** and **4**) and

Table 1. IC_{50} values of compounds **1**–**6** in three cell lines compared to the respective parent compounds with unsubstituted Cp (**P1**–**P6**)[18] and Cisplatin. IC_{50} values are means ± SDs from at least three independent experiments after continuous exposure for 96 h.

	CH1/PA-1 [μM]	SW480 [μM]	A549 [μM]
P1	> 200	> 200	> 200
P2	> 200	> 200	> 200
P3	151 ± 9	127 ± 18	75 ± 18
P4	> 200	> 200	> 200
P5	0.72 ± 0.13	1.6 ± 0.2	5.7 ± 1.0
P6	29 ± 10	55 ± 9	106 ± 15
1	30 ± 1	41 ± 6	64 ± 7
2	0.38 ± 0.08	0.89 ± 0.19	1.3 ± 0.1
3	13 ± 3	16 ± 4	34 ± 8
4	5.3 ± 1.1	16 ± 2	45 ± 8
5	0.11 ± 0.02	0.11 ± 0.02	0.14 ± 0.02
6	0.20 ± 0.03	0.33 ± 0.06	0.47 ± 0.12
Cisplatin[28]	0.073 ± 0.001	2.3 ± 0.2	3.8 ± 1.0

surprisingly high (**2**) activities. Moreover, the difference between the complexes containing the nontoxic maltolato and highly cytotoxic thiomaltolato ligands,[20] **(P)2**, **(P)6**, respectively, is less distinct in the lipophilic series, which indicates that the high activities are not solely due to the bioactive ligand. Also, while the thiomaltolato derivative is more active than the thioflavonato derivative in the parent series, this relation is inversed in the new series. To the best of our knowledge, compound **5** is the most active Mo compound in these cell lines published to date. In addition, the consistent activity in all three cell lines is also of interest, since the A549 cell line is usually most resistant to treatments, while the CH1/PA-1 is the most susceptible. This would indicate a mode of action of compound **5** which the cancer cells have difficulty defending in general.

For a basic insight into the mode of action, further experiments were performed with HCT116 colon carcinoma cells as well as with the corresponding bax and p53 knock-out sublines. Bax is a pro-apoptotic protein, which plays a major role in the regulation of the intrinsic (mitochondrial) pathway of apoptosis.[29] The tumor suppressor protein p53 is a key factor in cellular processing of DNA damage caused by anticancer agents, as it controls the regulation of cell cycle, cell death and DNA repair.[30] In the knock-out sublines, complex **1** exhibits 1.8 times (baxKO) and 1.5 times (p53KO) lower IC_{50} values than in the parental HCT116 cells. However, the three most cytotoxic molybdenocenes **2**, **5** and **6** showed negligible differences between their activities in the parental and the knock-out cell lines (Table 2, Figure S21). This strongly suggests that neither bax nor p53 are essential factors involved in the mechanisms of action.

Cellular accumulation

Cellular accumulation studies of complexes **1–6** were carried out in SW480 cells by measuring the total cellular molybdenum content by ICP-MS. Compound **1** bearing chlorido ligands showed only a low cellular uptake level (15 ± 1 fg [Mo]/cell) despite exposure to an extracellular concentration as high as 50 μM, which correlates very well with its moderate cytotoxicity. Cellular accumulation of the phthiocol derivative (**3**) turned out to be ten times higher (150 ± 14 fg [Mo]/cell), while uptake of compounds **2**, **4**, **5** and **6** even surpassed the latter by another three to four times, all at a treatment concentration of 50 μM (Figure 3). To obtain about 150 fg [Mo]/cell (Table S1), a ten times lower extracellular concentration (5 μM) was found sufficient for the maltol and thiomaltol complexes **2** and **6**. The high cellular accumulation of these and the thioflavone complex **5** correspond well with their low IC_{50} values and hence high cytotoxic potencies (Figure S22).

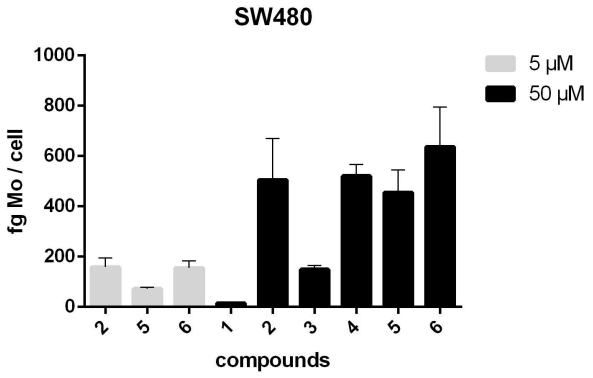

Figure 3. Cellular accumulation levels of molybdenum complexes in fg [Mo]/cell, measured by ICP-MS. SW480 cells were treated for 2 h at 37 °C with 50 μM of all test compounds (black columns) and with 5 μM of the more cytotoxic compounds **2**, **5** and **6** (grey columns). Values are means ± SDs from at least three independent experiments performed in triplicates.

Table 2. Cytotoxicity in three human carcinoma cell lines. Values are means ± SDs from at least three independent experiments after continuous exposure for 96 h.

	HCT116 [μM]	HCT116baxKO [μM]	HCT116p53KO [μM]
1	44 ± 2	24 ± 5	29 ± 5
2	0.85 ± 0.11	0.81 ± 0.12	0.84 ± 0.03
5	0.25 ± 0.03	0.22 ± 0.03	0.23 ± 0.03
6	0.42 ± 0.09	0.37 ± 0.06	0.38 ± 0.09

Apoptosis assay

Apoptosis induction was determined by flow-cytometric measurement of annexin V-FITC and PI (propidium iodide) double staining, allowing the quantification of viable, early- and late-stage apoptotic as well as necrotic cells. For these experiments we chose compounds **2**, **5** and **6**, which showed the highest activity in vitro, as well as the parent molybdenocene dichloride (**1**) for comparison purposes. SW480 cells were exposed to concentrations of 100 μM (**1**) or 5, 10, 15, 20 and 25 μM (**2**, **5** and **6**) and compared to untreated and positive controls. Table S2 summarizes the total percentages of early and late apoptosis in cells treated with the highest concentrations of the examined compounds. Furthermore, Figure 4 displays the concentration dependency of apoptosis induction of all tested compounds. Compounds **1** and **5** showed 19.0% and 13.9%, respectively, of early plus late apoptosis. The thiomaltol-containing compound **6** exhibited a greater apoptotic effect of 35.1% in total. The highest potency of apoptosis induction was observed for compound **2** containing the maltolato ligand at up to 79.3%. This ties in well with the unexpected activity of complex **2**, bearing the nontoxic maltolato ligand, in the MTT assay. The corresponding dot plots are shown in Figure S23.

Generation of reactive oxygen species

Generation of reactive oxygen species (ROS) is an important aspect in understanding the mechanisms of drugs, because both ROS-producing or -eliminating agents are used or being developed for treatment of cancer.[31] The ability of the compounds **1**, **2**, **5** and **6** to induce ROS production was investigated by the DCFH-DA assay. The dose-dependent

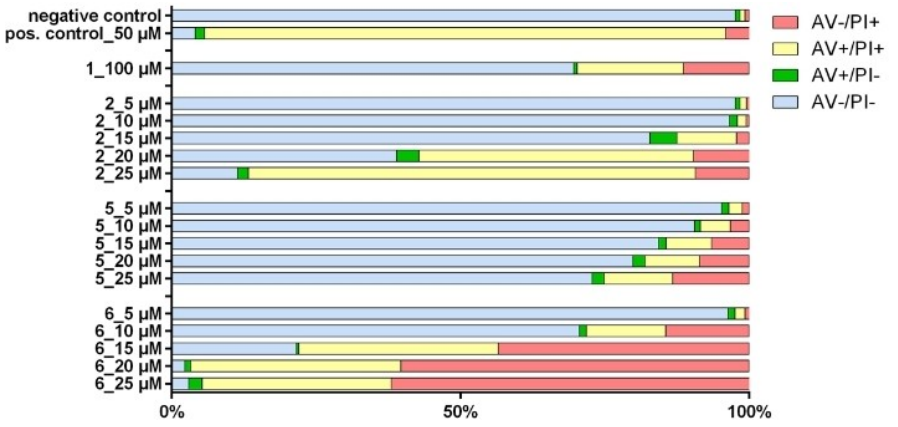

Figure 4. Fractions of viable (AV−/PI−), early apoptotic (AV + /PI−), late apoptotic (AV + /PI +) and necrotic (AV−/PI +) cells, measured by the flow-cytometric annexin V-FITC/PI assay upon treatment of SW480 cells with 100 µM of compound **1** or 5, 10, 15, 20 and 25 µM of compounds **2**, **5** and **6**.

increase of fluorescent DCF was measured over 2 h, and results are shown in Figure 5. All compounds show a negligible ROS generation within 2 h; however, a time dependence could frequently be observed, most pronounced at the highest concentration of 20 µM.

Proteomics experiments

Proteomic response profiles were evaluated after treating SW480 cancer cells with the parent compound **1** and the in vitro most active compound **5**. We used a label free quantification (LFQ) approach for protein quantification and comparison of cell responses upon different treatment conditions.[32] The response profiles were evaluated after a 24 h incubation. Therefore, the IC_{50} values after an incubation period of 24 h were initially elucidated. Compounds **1** and **5** yielded IC_{50} values of 44 µM and 0.11 µM, respectively, which are comparable to the 96 h incubation (see above). Both molybdenocenes were dissolved employing PVP as described above. The SW480 cancer cells were treated with compound **1** at 20 µM and with compound **5** at 0.1 µM for 24 h, after which the cells were lysed and the extracts were fractionated into cytoplasmic (CYT) and nuclear (NE) fractions according to previously published protocols.[33,34] The CYT contains the soluble protein fraction and the NE typically contains the

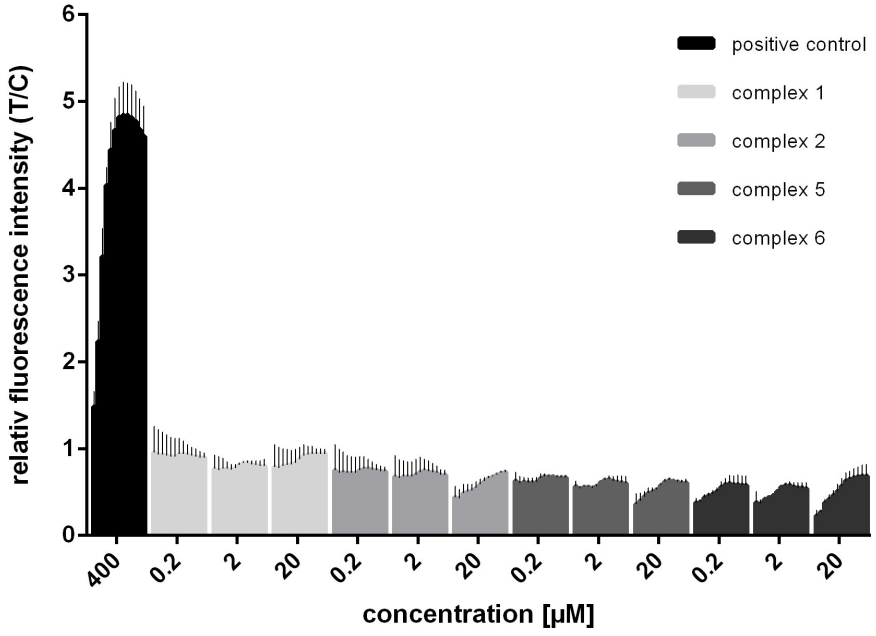

Figure 5. Reactive oxygen species production detected by the DCFH-DA assay in SW480 cells treated with 0.2, 2 and 20 µM of **1**, **2**, **5** and **6** for 2 h, measured every 10 min during incubation. Data are means ± SDs.

insoluble protein fraction, including nuclear and organellar proteins. After tryptic digestion of the proteins, peptide samples were analysed on a TimsTOF pro mass spectrometer. The treatment of cells, as well as the vehicle controls (i.e., cells treated with PVP only) were carried out in hexuplicates. A total of 5488 proteins were identified. Scatter plots revealed an acceptable correlation among the replicates on the protein level, with correlation coefficients typically >0.8 (Figure S24 A). A list of all the identified proteins in SW480 cancer cells treated with **1** or **5** can be found in Supporting Information Table Proteomics, including significances.

When compared to vehicle-treated cells, the treatment with the molybdenocenes featured distinct protein regulations (Figures 6 and S24 B). Compound **1** displayed 253 significant-protein regulations in the NE fraction, while 7 proteins were significantly regulated in the CYT fraction (Figure 6 A). Compound **5** led to a considerable number of significant protein regulations in CYT (427) and NE (1517) fractions. Significances were calculated with a false-discovery rate (FDR) 0.05 and $S0=0.1$ (see Experimental Section). The parent molybdenocene dichloride **1** affected preferentially the NE fraction, while the thioflavonato molybdenocene **5** perturbed both CYT and NE fractions. Despite these differences, two proteins in the CYT fraction and 109 proteins in the NE fraction were similarly regulated by both treatments (Figure S24 B). Of these, tubulin-associated (Benjamini-corrected p-value $=5\times10^{-2}$) and mitochondrial inner membrane proteins (Benjamini-corrected p-value $=2.5\times10^{-7}$) were significantly down-regulated by both treatments (Figure 7 A). This is paralleled by a uniform upregulation of myosin-related proteins, which involve the myosin complex and myosin stress fibers (Figure 7 A). The proteome effects of **5** on SW480 cancer cells were evaluated in more detail by the functional annotation tool using the DAVID bioinformatics resource.[35,36] Significantly regulated proteins in the CYT and NE fractions were analysed for enriched KEGG pathways and gene ontology terms according to biological processes and cellular compartments. Enriched pathways and terms with a significant Benjamini-corrected p-value <0.05 were considered for further evaluation. Moreover, redundant pathways and terms were combined to a single term. The

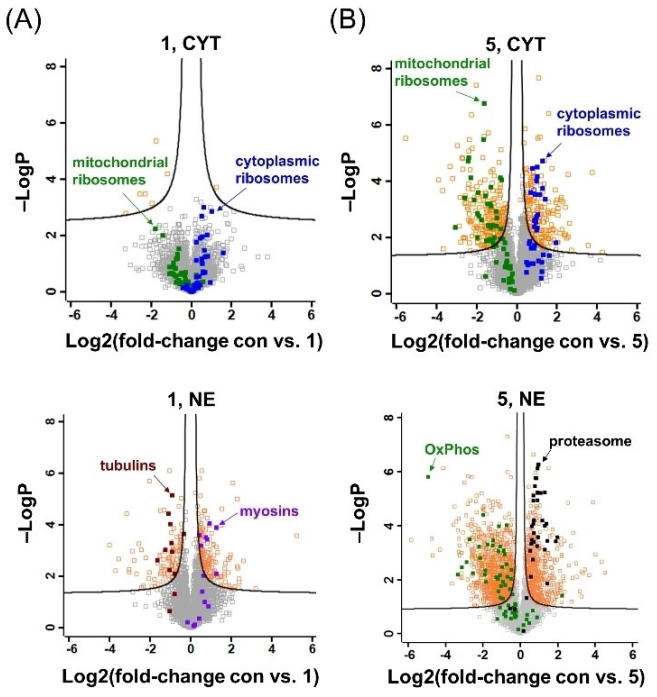

Figure 6. Proteomic analysis of the cellular response of SW480 cancer cells to treatment with A) compound **1** and B) **5**. The volcano plots illustrate the significantly regulated proteins as orange squares. Notable protein groups were additionally coloured. The *x*-axis depicts Log2 fold-changes of LFQ protein abundance between control and treatment and the y-axis depicts the significance of the regulation in Log10-scale.

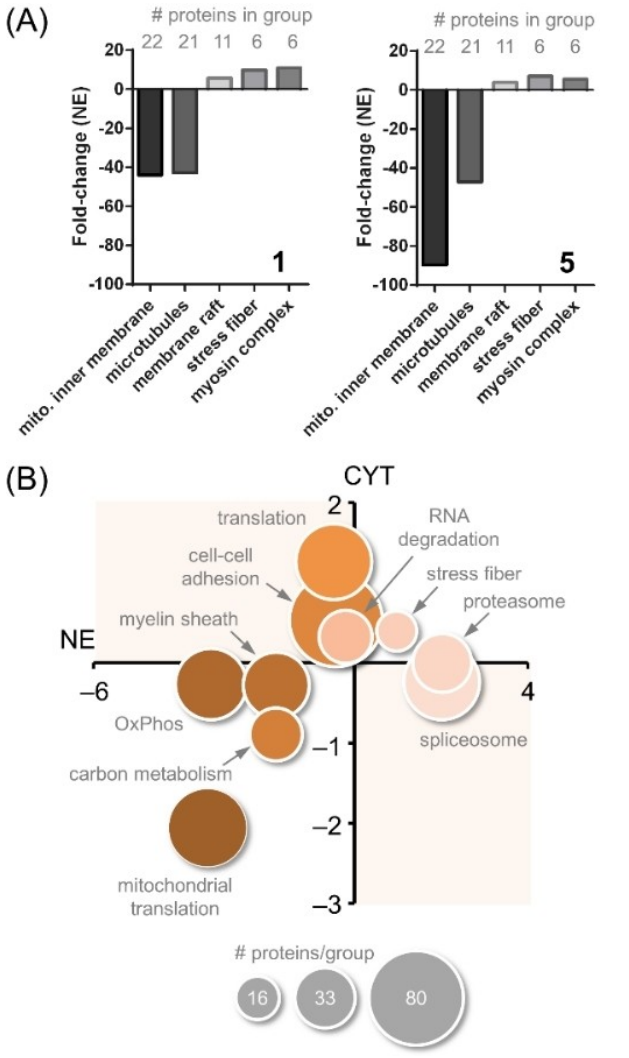

Figure 7. Regulation of functional protein groups in SW480 cancer cells upon treatment with compound **1** or **5**. A) Similar protein regulations upon treatment with **1** (left) or **5** (right) are associated with mitochondrial inner membrane proteins, microtubules, membrane raft, stress fiber and myosin complex. The bars represent the summed fold-change of the proteins in each group. Only proteins from the NE fraction were considered. B) The global cellular response to the treatment with **5** is depicted. The ten most significantly regulated functional protein groups are shown. Each bubble represents a labelled functional protein group and its position is determined by the average protein fold-change in the NE (*x*-axis) and CYT (*y*-axis) fractions. The size of the bubble represents the number of proteins in each group. OxPhos = oxidative phosphorylation of the cellular respiration.

average protein fold-change in each protein group was then calculated for both the CYT and NE fractions. The ten most strongly regulated protein groups are visualized in Figure 7 B. The size of the bubbles represents the number of proteins in each group, which consist of a total of 434 proteins. Their compositions can be found in the source data to Figure 7 (Supporting Information). This regulome provides insight into the global cellular response of SW480 cells to the treatment with compound **5**. Of note, stress fiber proteins were upregulated in CYT and NE fractions, while ribosomal proteins (translation) and proteins involved in cell-cell adhesion were mainly upregulated in the CYT fraction. Interestingly, many proteasomal components were upregulated in the nucleus and indicate a cellular response to ROS stress in the nucleus.[37] This is paralleled by a similar upregulation of spliceosomal proteins. Mitochondrial proteins included in mitochondrial translation and oxidative phosphorylation (OxPhos) were down-regulated in both CYT and NE fractions (see also Figure 6 B) as were proteins involved in myelin sheath formation. The cytoplasmic downregulation of mitochondrial ribosomes and the concomitant upregulation of cytoplasmic ribosomes was a striking feature of treating SW480 cancer cells with compound **5** (Figure 6 B) and suggest a strong impact of the molybdenocene on translation in these cells. Treatment with **5** also seemed to down-regulate proteins involved in carbon metabolism and consequently, many components related to glycolysis, the pentose phosphate pathway (PPP), the citrate cycle and fatty acid degradation were down-regulated (Figure S24 C). Although most components were down-regulated, some key proteins connecting glycolysis to the PPP and to the citrate cycle were upregulated, namely glucose-6-phosphate dehydrogenase (G6PD) and pyruvate kinase (PKM), respectively. Upregulation of G6PD might increase the capacity of the cells to generate reducing equivalents and is implicated in cancer resistance against cisplatin[38] or erlotinib[39] amongst others. In contrast to previous experiments, compound **5** did not lead to a significant regulation of heme oxygenase-1 (HMOX1), which is often upregulated when exposing cancer cells to ROS-inducing metallodrugs.[40] In fact, compound **5** exhibited anti-oxidant behaviour. With respect to redox-related proteins, we found thioredoxin reductase 1 (TXNRD1) and microsomal glutathione S-transferase 2 (MGST2) significantly upregulated upon treatment with **5**, while other proteins involved in redox control were down-regulated, for example NQO1, SOD1, GPX8, HAGH, GPX4 and GLO1 (Figure S25). While these redox proteins were largely down-regulated, several heat shock proteins were significantly up-regulated in both CYT and NE. This includes the classical heat shock proteins HSPA8 and HSPA1 A, whereas the HSPA1 A-inhibitor HSPBP1 was down-regulated (Figure S25).

Overall, the molybdenocene moiety seemed to relate to perturbations in myosin/tubulin networks and proteins located in the inner mitochondrial membrane. The latter involves the NADH:ubiquinone oxidoreductase and cytochrome c oxidase complexes, corresponding to complexes I and III of the respiratory chain, respectively. In contrast, the thioflavonato complex **5** featured additional drug effects on the proteome level. The most striking features include the down-regulation of mitochondrial proteins and the up-regulation of proteasomal proteins in the NE fraction. Finally, redox related proteins were rather down-regulated, together with up-regulated heat shock proteins may be directly related to the anti-oxidant effects of compound **5** in SW480 cancer cells.

In vivo experiments

Compounds **1** and **5** were chosen for in vivo evaluation in CT26 allograft (s.c.) bearing Balb/c mice. Compound **5** was selected due to its high in vitro efficacy while compound **1** was selected because it is the most structurally similar to molybdenocene dichloride (Cp_2MoCl_2), which has already been tested in vivo, showing promising results.[2]

Compound **1** was administered at 5 mg/kg, i.p., three times a week and showed no activity, rather a non-significant increase in tumour volume was noted when compared to the control group (Figure 8 A and B). Compound **5** was administered at 1 mg/kg, i.v., three times a week, the difference in administration route and dosage being in consequence to toxic side effects noted in i.p. application. At this dosage, compound **5** showed significant tumour growth delay (Figure 8 C and D), although there was little effect on overall survival.

Organ distribution of compound 5

In order to gain insight into the organ distribution of compound **5**, Mo levels in heart, lung, liver, kidney, spleen and blood of four mice which had been treated with compound **5** as part of a toxicity experiment were determined by ICP-MS. The mice had been administered 1 mg/kg injections of compound **5** on three consecutive days (two mice were treated i.p., two were treated i.v.) and the organs were harvested two days after the last treatment. In order to account for naturally occurring Mo, the results were compared to one untreated mouse. The results are summarized in Table S3. The mice which were treated with compound **5** show elevated Mo levels in all organs except the liver, where the treatment decreased Mo levels significantly. The Mo content of the spleen is decreased for i.v. injected mice, while the i.p. injected mice show elevated concentrations compared to the control mouse and almost double the levels of i.v. treated mice. Mo levels higher than the limit of quantification in the blood were only found in one i.p treated mouse. We are unaware of any reports of molybdenum organ distribution studies and have undertaken these experiments to enable comparisons with future studied molybdenum anticancer agents. However, due to the small sample size, these findings should be considered cautiously.

Conclusion

We have synthesized, characterized and thoroughly investigated the anticancer activity, both in vitro and in vivo, as well as through proteomics experiments, of a series of lipophilic

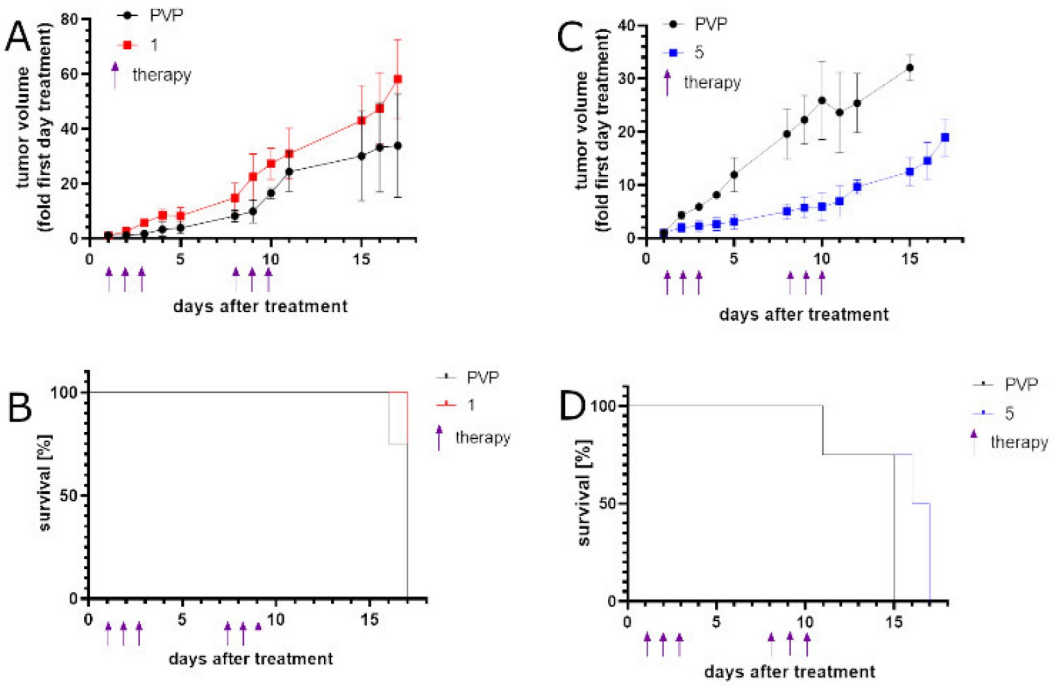

Figure 8. In vivo anticancer activity of compounds **1** and **5**; A and C) depict average tumor volumes over time, B and D) show overall survival of mice.

diphenylmethyl substituted-Cp molybdenocenes. Compound **5**, containing a thioflavonato ligand, exhibits the highest activity against cancer cells in vitro, with IC_{50} values in the submicromolar range in all three cancer cell lines (human ovarian teratocarcinoma CH1/PA1, human colon cancer SW480, human non-small lung cancer A549) and is the most active molybdenum complex reported, to our knowledge. Furthermore, in vivo experiments showed compound **5** to significantly inhibit tumour growth, however, no significant increase in life expectancy was observed.

The diphenylmethyl substitution of the Cp moieties greatly increases (up to 400 times) the cytotoxicity when compared with the non-substituted Cp_2MoL analogs. The increase in lipophilicity definitely plays a large role in the high cellular uptake and is in turn increasing the anticancer activity. Structure activity relationships of the ligands when comparing the cytotoxicity in all three cell lines follow this trend: thioflavonato > thiomaltolato > maltolato ≫ phthiocol/picolinato > dichlorido. The (S,O)- coordinated ligands themselves possessing a higher toxicity than their (O,O)- coordinated counterparts would explain this trend. However, the bioactive chelating ligand cannot be solely responsible for the anticancer activities since compound **2**, containing the non-cytotoxic maltol ligand, also shows micromolar and submicromolar IC_{50} values. The general decrease in ligand lipophilicity results in a decrease in activity in the complexes.

The mode of action of these compounds was also investigated and showed that ROS generation was not observed for any compounds in the series. Proteomics experiments with compound **5** confirmed this result, actually showing antioxidative affects. The intrinsic (mitochondrial) pathway to apoptosis as well as DNA damage were both ruled out by bax and p53 knockout cell lines, respectively. Apoptosis assay also confirmed this in compounds **1**, **5** and **6**, which produced very few apoptotic cells. Interestingly, compound **2** is the only one of the series that showed significant apoptosis (79.3 %) which would indicate a different mode of action than that of the others.

Proteomics showed that compound **5** regulated eight times the number of proteins in the cytoplasmic (427) and nuclear fraction (1517) combined as parent molybdenocene **1** (7 and 253, respectively), suggesting that the thioflavonato ligand plays an important role in the mode of action in the cells. Both compounds **1** and **5** demonstrated a significant regulation of tubulin-associated and mitochondrial inner membrane proteins and compound **5** showed a strong metabolic effect.

We believe molybdenocenes to have great potential as anticancer agents; the key is to find a balance, greater lipophilicity results in higher uptake and generally increased anticancer activity. In our case this resulted in great in vitro results, but when employed in vivo the toxicity of compound **5** caused problems in the application method as well as yielding mixed results, on one hand tumour growth was significantly slowed but on the other life expectancy did not increase. Further experiments to optimise the activity and shed more light onto the mode of action of this promising class of compound are continuing.

Experimental Section

Materials and methods

Cell lines and culture conditions: Human CH1/PA-1 (kindly provided by Lloyd R. Kelland, CRC Centre for Cancer Therapeutics, Institute of Cancer Research, Sutton, UK; confirmed by STR profiling as PA-1 ovarian teratocarcinoma cells at Multiplexion, Heidelberg, Germany), SW480 colon carcinoma and A549 non-small cell lung cancer cells (both obtained from ATCC) were maintained in minimal essential medium (MEM) supplemented with 1 mM sodium pyruvate, 4 mM l-glutamine, 1% (v/v) non-essential amino acids from 100-fold stock (all purchased from Sigma-Aldrich) and 10% heat-inactivated fetal bovine serum (BioWest). Human HCT116 colon carcinoma cells (from ATCC) as well as the two sublines HCT116 bax-ko and HCT116 p53-ko (both kindly provided by Bert Vogelstein, Ludwig Center at Johns Hopkins University, Baltimore, MD, USA) were cultured in RPMI 1640 medium (Sigma-Aldrich) supplemented with 4 mM L-glutamine and 10% heat-inactivated fetal bovine serum. Cells were grown as monolayers in 75 cm^2 culture flasks (Starlab) at 37 °C in a humidified atmosphere containing 5% CO_2.

Cytotoxicity assay: Cytotoxicity of the compounds was determined by means of a colorimetric microculture assay (MTT assay). Cells were harvested from culture flasks by trypsinization and seeded into 96-well microculture plates (Starlab) in densities of 1×10^3 CH1/PA-1, 2×10^3 HCT116 (including sublines) as well as SW480 and 3×10^3 A549 cells per well (each in 100 μL). After a 24 h drug-free preincubation, cells were exposed to serial dilutions of the test compounds for 96 h. Dry 1:10 co-precipitates of the test compounds with polyvinylpyrrolidone (PVP, Sigma-Aldrich) were dissolved and serially diluted in the appropriate complete medium (depending on the cell line), and each dilution was added to plates in triplicates (100 μL/well). At the end of the exposure, the drug-containing media were replaced with 100 μL of a RPMI 1640/MTT mixture. For this purpose, MTT (3-(4,5-dimethylthiazol-2-yl)-2,5-diphenyl-2H-tetrazolium bromide) solution was prepared in phosphate-buffered saline (5 mg/mL) and mixed with complete RPMI 1640 medium in a volume ratio of 1:6. After incubation for 4 h, these mixtures were removed, and the formazan products were dissolved in 150 mL of DMSO per well. Optical densities at 550 nm (and at 690 nm as a reference) were measured with a microplate reader (BioTek ELx808). The 50% inhibitory concentrations (IC_{50}) relative to untreated controls and were interpolated from concentration-effect curves. At least three independent experiments were performed.

Cellular accumulation: SW480 cells were seeded at densities of 1.8×10^5 cells/well into 12-well plates in a total volume of 1 mL per well in complete MEM. (The same number of cells were seeded into three wells of a parallel plate for determination of the cell number on the day of treatment.) After 24 h the cells were exposed to 5 μM or 50 μM of the test compounds (**1**–**6**) in complete MEM and incubated at 37 °C for 2 h. After the 2 h incubation, the medium was removed, and the cells were washed with 3×1 mL PBS. After the last washing step PBS was removed completely and the cells were lysed by addition of 400 μL HNO_3 per well for 1 h at room temperature. Molybdenum content was quantified by ICP-MS in dilutions of the samples to a total volume of 8 mL (300 μL sample + 7.7 mL MilliQ water). The measured amount of accumulated metal was normalised to the cell number. Results are presented as fg [Mo]/cell averaged from at least three independent experiments.

An Agilent 7800 ICP-MS instrument (Agilent Technologies, Tokyo, Japan) equipped with an Agilent SPS 4 autosampler (Agilent Technologies, Tokyo, Japan) was used to determine the molybdenum content. The ICP-MS parameters were tuned on a daily base to achieve high sensitivity. The ICP-MS was equipped with a MicroMist nebulizer with a sample uptake rate of ~0.25 mL min^{-1} and standard nickel cones. The Agilent MassHunter software package (Workstation Software, Version C.01.06, 2019) was used for data evaluation. The instrumental parameters are listed in Table S4.

Annexin V/PI assay: Induction of apoptotic and necrotic cell death was quantitatively analyzed via flow cytometry upon double staining with FITC-conjugated annexin V (BioVision) and propidium iodide (PI, Fluka). SW480 cells were seeded into 24-well plates (7×10^4 cells/well) in 600 μL MEM. After a 24 h incubation, cells were exposed to 100 μM of compound **1** or a range of concentrations (5–25 μM) of compounds **2**, **5** and **6** for 24 h. After treatment, the drug-containing medium was collected, cells were washed once with 37 °C warm PBS, and trypsinized for 5 min. Following trypsinization, the cell suspension was added to the pre-collected medium and cells were pelleted by centrifugation (300 g, 3 min). The supernatant was discarded and the cell pellet resuspended with 1.5 μL FITC-conjugated annexin V (Thermo Fisher, Catalog# BMS306FI-300) in 150 mL binding buffer (10 mM HEPES/NaOH pH 7.4, 140 mM NaCl, 2.5 mM CaCl2) and incubated at 37 °C for 15 min. Propidium iodide (3.3 μg/mL) was added shortly before analysis using a Guava easyCyte BHT instrument (Merck Millipore, Burlington, MA, USA) with InCyte software. Results were quantified by using the FlowJo software (Tree Star). At least three independent experiments were performed.

dsDNA plasmid interaction studies: Stock solutions of the test compounds (**1**, **2**, **5** and **6**) were prepared in MilliQ water. 400 ng of the pUC19 plasmid (2686 bp) were incubated with the test compounds at a final concentration of 50 μM. For detection of changes in DNA secondary structure, the incubation was performed for different time intervals (15 min to 6 h) with continuous shaking at 37 °C. 4 μL aliquots of 6× DNA loading dye were added to the 20 μL DNA samples and the reaction products were separated in a 1% agarose gel in 1×TBE buffer. The electrophoresis was initiated at 60 V for 5 min and continued at 120 V for 90 min. For visualization of the DNA modification degree, the agarose gel was stained with ethidium bromide (EtBr) in 1× TBE (0.75 μg/ml) for 20 min. Images were taken by the GelDoc-It Imaging System Fusion Fx7 (Vilber Lourmat). For quantification of the spots, ImageJ/Fiji1.46 was used.

DCFH-DA assay: SW480 cells were seeded into 96-well plates (2.5×10^4 cells/100 μL/well). After 24 h the cells were washed with 200 μL Hanks' balanced salt solution (HBSS, Sigma-Aldrich), to which 1% FCS had been added, and incubated with 100 μL of 25 μM 2',7'-dichlorofluorescein diacetate (Sigma-Aldrich) in HBSS (with 1% FCS) for 45 min at 37 °C. At the end of the incubation period, DCFH-DA solution was removed, and cells were washed with 200 μL HBSS. Cells were exposed to the test compounds (**1**, **2**, **5** and **6**) at a range of concentrations (0.2–200 μM) in 200 μL phenol-red-free MEM (Gibco; with 1% FCS) in triplicates. Fluorescence emission was measured at 10 min intervals with the BioTek Synergy HT reader (Excitation: 485/20 nm, Emission: 516/20 nm) over a 2 h period. All experiments included blanks (phenol-red-free medium with 1% FCS), negative controls (non-drug-treated cells) and positive controls (cells treated with 200 μM and 400 μM tert-butylhydroperoxide (Sigma-Aldrich)).

Proteomics analysis: *Cell culture and sample preparation*: SW480 cells were seeded at densities of 2×10^6 cells/well into T25 flasks for adherent cells in complete MEM. The cells were left to adhere for 24 h. Then, the medium was replaced and the cells were exposed to 20 μM and 0.1 μM of compounds **1** and **5**, respectively, for 24 h. The molybdenocenes were solubilized with PVP and stock solutions prepared in DMSO, which were immediately used by diluting in complete medium. Control cells were treated with PVP in DMSO.

Each condition was performed in six biological replicates. Then, the samples were fractionated into cytoplasmic (CYT, soluble) and nuclear extract (NE, insoluble) fractions as previously reported[33, 34]. In brief, the cells were thoroughly washed with PBS, lysed with isotonic lysis buffer (containing protease and phosphatase inhibitors) by applying shear stress. Membrane rupture was checked under a microscope. The nuclei were centrifuged and the supernatant (CYT) containing the soluble proteins was precipitated in ethanol at −20 °C. The cellular nuclei were lysed under hypertonic conditions and by means of sonication. After another centrifugation step to remove remaining DNA, the NE fraction in the supernatant was also precipitated in ethanol at −20 °C. The protein fractions were pelleted, dried and solubilised in sample buffer (7.5 M urea, 1.5 M thiourea, 4% CHAPS, 0.05% SDS and 100 mM dithiothreitol) before the total protein amount was determined by means of a colorimetric Bradford assay. A total of 20 μg protein per sample were then tryptically digested. This involved reduction with dithiothreitol, alkylation with iodoacetamide and digestion with trypsin/Lys-C according to a filter-assisted protein digestion (FASP) protocol.[33,34] The obtained peptide samples were dried in a speed-vac.

Data acquisition and analysis: The dried peptide samples were reconstituted in formic acid (5 μL, 30%) including four synthetic peptide standards (10 fmol each). They were topped up with eluent A (40 μL, 97.9% H_2O, 2% acetonitrile with 0.1% formic acid). The samples were analysed by nLC-MS/MS using a Dionex Ultimate 3000 nano-LC (Thermo Fisher Scientific, Bremen, Germany) coupled to a timsTOF pro mass spectrometer (Bruker Daltonics, Bremen, Germany). The injection volume was 1 μL and the flow rate was 300 nL min^{-1}. The peptide samples were injected on a trapping column (Pepmap100 precolumn, 2 cm × 100 μm, C18, Thermo Fisher Scientific) and separated on an Aurora emitter column (25 cm × 75 μm, C18, Ionoptics). Each analysis was based on a 90 min gradient from 8–40% eluent B (79.9% acetonitrile, 20% H_2O with 0.1% formic acid) using the PASEF mode (10 PASEF cycles). We used a cycle time of 1.16 s and target intensity threshold of 2,500. The raw data was searched and analysed performing label-free quantification (LFQ) using MaxQuant (version 1.6.17.0). A false-discovery rate (FDR) of ≤0.01 on protein and peptide level was selected, including a maximum of two missed cleavages per peptide. Identifications were based on at least one unique peptide per protein. The peptide mass tolerances were 50 ppm and 25 ppm for the first and main searches, respectively. Carbamidomethylation was chosen as a fixed modification on cysteines and methionine-oxidation, as well as N-terminal acetylation as variable modifications. The option "match between runs" was selected. MaxQuant analysed 536,090 full mass spectra and 1,885,316 MS^2 mass spectra. The MaxQuant output files were further processed and analysed by Perseus (version 1.6.6.0) to perform statistical analysis. Multi-parameter-corrected significant protein regulations were obtained using FDR ≤ 0.05 and S0 = 0.1.

In vivo experiments: Eight-to nine-week-old female BALB/c mice were bread in house (originally obtained from Harlan Laboratories (San Pietro al Natisone, Italy)) and were kept in pathogen-free conditions and controlled environment with 12 h light-dark cycle. CT26 (5×10^5 in 50 μL serum-free RMPI medium) cells were injected into the right flank of female BALB/c mice. When all tumors were measurable (at day 5), all animals were treated with solutions of **1** (5 mg/kg i.p.) and **5** (1 mg/kg, i.v.) (100 μL per 20 g, dissolved in ddH_2O). The control groups received solvent-PVP (100 μL per 20 g, ddH_2O). Tumor growth was evaluated by daily recording of tumor size by caliper measurement. Animals were sacrificed by cervical dislocation. In case of organ distribution studies, blood was drawn by cardiac puncture under deep, terminal anesthesia followed by cervical dislocation, dissection, and organ removal. All procedures were performed in a laminar flow hood. All animal experiments were performed according to FELASA guidelines and under consideration of the "3R principle" in animal experimentation (replacement, reduction, and refinement). The experiments were approved by the Federal Ministry of Education, Science and Research (BMBWF) under the reference number BMBWF-66.009/0157-V/3b/2019 after review and approval by the Ethics Committee for the Care and Use of Laboratory Animals at the Medical University Vienna.

Organ distribution: Samples were prepared from mouse blood and organs as published.[41] An Agilent 7800 ICP-MS instrument (Agilent Technologies, Tokyo, Japan) equipped with an Agilent SPS 4 autosampler (Agilent Technologies, Tokyo, Japan) was used to determine the molybdenum content. The ICP-MS was equipped with standard nickel cones. The Agilent MassHunter software package (Workstation Software, Version C.01.04, 2018) was used for data evaluation. The limit of quantification (LOQ) was determined using six digestion blanks as LOQ = 10*stdev = 0.053 ng/g. The instrumental parameters and digestion conditions can be found in Tables S4 and S5.

Syntheses: All manipulations involving moisture- and air sensitive chemicals were performed using a combination of glove box and Schlenk techniques.

2-Hydroxy-3-methyl-1,4-naphthoquinone,[42] 2-(4-chlorophenyl)-3-hydroxy-4*H*-chromene-4-thione[43,18] and thiomaltol[44] were synthesized according to literature procedures.

Sodium methoxide, granunlar tin, menadione, picolinic acid, Lawesson's reagent, 2′-hydroxyacetophenone, 4-chlorobenzaldehyde (Acros-Fisher), sodium hexafluorophosphate, molybdenum(V) chloride (Alfa Aesar), super hydride solution (1 M in THF), 6,6-diphenylfulvene, maltol (Sigma-Aldrich), Hydrogen Peroxide solution (30%), sodium carbonate, magnesium sulfate (Fisher Scientific), and H_2SO_4 (VWR International) were purchased from commercial sources and used as received.

Analyses: Cyclovoltammetric measurements were conducted using an EG & G PARC 273 A potentiostat/galvanostat using 3 mM solutions in DMF with [n-Bu_4N][BF4] (0.2 mM) as a supporting electrolyte. A platinum wire (CH Instruments) was used as auxiliary electrode, a Ag/Ag+ reference electrode containing 0.10 M $AgNO_3$ (CH Instruments) and a glassy carbon electrode (CH Instruments) as working electrode. The solutions were degassed by passing an Argon stream through them for 5 minutes prior to measurements. Ferrocene was used as an internal standard. Data was collected at a scan rate of 200 mV s^{-1}. Measurements were performed in triplicate, the third cycle is plotted.

UV/Vis spectra were recorded on a PerkinElmer LAMBDA 35 UV/Vis spectrometer.

NMR spectra were measured on a Bruker Avance III™ 500 MHz spectrometer. DMSO-d_6 was used as solvent for all compounds except **3** which was not stable in DMSO, therefore $CDCl_3$ was used despite the solvent peak partially overlapping with aromatic signals.

Elemental analyses were measured at the Microanalytical Laboratory of the University of Vienna with a Perkin-Elmer 2400 CHN Series II elemental analyser or a Eurovector EA3000 elemental analyser.

The X-ray intensity data were measured on Bruker D8 Venture diffractometer equipped with multilayer monochromator, Mo K/α INCOATEC micro focus sealed tube and Oxford cooling system. The structures were solved by *Structure Expansion and Direct Methods.* Non-hydrogen atoms were refined with *anisotropic displacement*

parameters. Hydrogen atoms were inserted at calculated positions and refined with riding model. The following software was used: Bruker SAINT software package[45] using a narrow-frame algorithm for frame integration, SADABS[46] for absorption correction, OLEX2[47] for structure solution, refinement, molecular diagrams and graphical user-interface, Shelxle[48] for refinement and graphical user-interface SHELXS-2015[49] for structure solution, SHELXL-2015[49] for refinement, Platon[50] for symmetry check.

Synthetic procedures

General procedure for the synthesis of complexes 2–6: Ligand (1.2 eq.) and NaOMe (1.4 eq.) were dissolved in dry MeOH (24 mL) and stirred at room temperature under argon for 10 minutes. In a separate Schlenk flask, compound **1** (100 mg, 0.16 mmol, 1 eq.) was dissolved in dry dichloromethane (8 mL), the prior solution was added via cannula and the resulting mixture was stirred at room temperature for 20 h. Work-up was performed open to air: $NaPF_6$ (2 eq.) was added and the mixture was stirred for another 2 h. Then, the solvents were removed under reduced pressure, the residue was extracted into dichloromethane, washed with water (3×20 mL), dried over $MgSO_4$ and filtered through a folded filter. The solution was concentrated to 2 mL and the product was precipitated through the addition of Et_2O, filtered, washed with n-hexane and dried in vacuo.

Compound 1: *Bis[η^5-1-(diphenylmethyl)cyclopentadienyl] dichloridomolybdenum(IV).* In a three times flame dried Schlenk tube, super hydride (15.6 mL, 1 M in THF, 1.2 eq.) was added to 6,6-diphenylfulvene (3 g, 13 mmol, 1 eq.) and the mixture was stirred at room temperature for one hour. The solvent was removed in vacuo (first at ambient temperature, later at 90 °C) affording a colorless solid, and granular Sn (2.16 g, 18.2 mmol, 1.4 eq.) and $MoCl_5$ (2.13 g, 7.8 mmol, 0.6 eq.) were added. The solids were suspended in dry diethyl ether (40 mL), sonicated for 5 minutes and stirred at ambient temperature for 24 h.

Work-up was performed open to air: the solvent was removed *in vacuo* and the residue was extracted into DCM and filtered through celite. The filtrate was concentrated under reduced pressure and the residue was purified by means of column chromatography (EtOAc/n-hexane = 1 : 2–2 : 1, slow gradient).

Yield: 12 %, greyish-green solid. ^{1}H NMR (500.10 MHz, DMSO-d6) δ = 7.29–7.25 (m, 8H), 7.23–7.19 (m, 12H), 5.19 (s, 2H), 4.91 (t, *J* = 2.5 Hz, 4H), 4.74 (t, *J* = 2.5 Hz, 4H) ppm. (ESI$^+$) m/z: $[M–Cl]^+$ = 595.18, $[M–Cl]AcN^+$ = 636.20; calculated: 595.11, 636.14; Elemental analysis calculated for $C_{36}H_{30}Cl_2Mo$: C: 68.69 %, H: 4.80 %; found: C: 68.67 %, H: 4.90 %;

Compound 2: *Bis[η^5-1-(diphenylmethyl)cyclopentadienyl] [3-(oxo-κO)-2methyl-4H-pyran(4-oato-κO)] molybdenum(IV) hexafluorophosphate.* The synthesis was carried out according to the general procedure using 25 mg maltol (0.19 mmol, 1.2 eq.), 13 mg NaOMe (0.24 mmol, 1.4 eq.), 100 mg **1** (0.16 mmol, 1 eq.) and 54 mg $NaPF_6$ (0.32 mmol, 2 eq.).

Yield: 65 %, brown solid. ^{1}H NMR (500.10 MHz, DMSO-d6) δ = 8.43 (d, *J* = 5.1 Hz, 1H), 7.34–7.17 (m, 20H), 6.96 (d, *J* = 5.1 Hz, 1H), 5.84 (dd, *J* = 4.8, 3.0 Hz, 2H), 5.28 (dd, *J* = 5.3, 2.8 Hz, 2H), 5.15 (dd, *J* = 4.9, 2.4 Hz, 2H), 4.66 (dd, *J* = 4.4, 2.3 Hz, 2H), 4.58 (s, 2H), 2.70 (s, 3H) ppm. (ESI$^+$) m/z: $[M]^+$ = 685.22; calculated: 685.16; Elemental analysis calculated for $C_{42}H_{35}O_3MoPF_6$: C: 60.88 %, H: 4.26 %; found: C: 60.61 %, H: 4.52 %;

Compound 3: *Bis[η^5-1-(diphenylmethyl)cyclopentadienyl] [2-(oxo-κO)-3-methylnaphthalene-1,4-dione(4-oato-κO)] molybdenum(IV) hexafluorophosphate.* The synthesis was carried out according to the general procedure using 34 mg 2-Hydroxy-3-methyl-1,4-naphthoquinone (0.19 mmol, 1.2 eq.), 13 mg NaOMe (0.24 mmol, 1.4 eq.), 100 mg **1** (0.16 mmol, 1 eq.) and 54 mg $NaPF_6$ (0.32 mmol, 2 eq.).

Yield: 52 %, purple solid. ^{1}H NMR (500.10 MHz, $CDCl_3$) δ = 8.09 (d, *J* = 7.0 Hz, 1H), 7.93–7.83 (m, 2H), 7.68 (t, *J* = 7.1 Hz, 1H), 7.29–7.15 (m, 20H, partially superposed by solvent signal), 6.24 (br s, 2H), 5.24–5.22 (m, 4H), 4.68 (br s, 2H), 4.66 (s, 2H), 2.44 (s, 3H) ppm. (ESI$^+$) m/z: $[M]^+$ = 747.23; calculated: 747.18; Elemental analysis calculated for $C_{47}H_{37}O_3MoPF_6$: C: 63.38 %, H: 4.19 %; found: C: 63.47 %, H: 4.25 %;

Compound 4: *Bis[η^5-1-(diphenylmethyl)cyclopentadienyl][2-(carboxylato-κO)-pyridine-κN] molybdenum(IV) hexafluorophosphate.* The synthesis was carried out according to the general procedure using 20 mg picolinic acid (0.19 mmol, 1.2 eq.), 13 mg NaOMe (0.24 mmol, 1.4 eq.), 100 mg **1** (0.16 mmol, 1 eq.) and 54 mg $NaPF_6$ (0.32 mmol, 2 eq.).

Yield: 73 %, brown solid. ^{1}H NMR (500.10 MHz, DMSO-d6) δ = 8.34 (d, *J* = 5.4 Hz, 1H), 8.23 (td, *J* = 7.7, 1.3 Hz, 1H), 8.05 (dd, *J* = 7.7, 1.0 Hz, 1H), 7.61 (ddd, *J* = 7.4, 5.6, 1.5 Hz, 1H), 7.32–7.28 (m, 8H), 7.27–7.18 (m, 12H), 6.30 (dd, *J* = 4.6, 3.0 Hz, 2H), 5.34 (dd, *J* = 5.5, 2.8 Hz, 2H), 5.22 (dd, *J* = 5.0, 2.5 Hz, 2H), 4.76 (d, *J* = 1.8 Hz, 2H), 4.63 (s, 2H) ppm. (ESI$^+$) m/z: $[M]^+$ = 682.22; calculated: 682.16; Elemental analysis calculated for $C_{42}H_{34}NO_2MoPF_6$: C: 61.10 %, H: 4.15 %, N: 1.70 %; found: C: 60.85 %, H: 4.10 %, N: 1.68 %;

Compound 5: *Bis[η^5-1-(diphenylmethyl)cyclopentadienyl] [3-(oxo-κO)-2-(4′ chlophenyl) chromen-(4-thioato-κS)] molybdenum(IV) hexafluorophosphate.* The synthesis was carried out according to the general procedure using 55 mg 2-(4-chlorophenyl)-3-hydroxy-4H-chromene-4-thione (0.19 mmol, 1.2 eq.), 13 mg NaOMe (0.24 mmol, 1.4 eq.), 100 mg **1** (0.16 mmol, 1 eq.) and 54 mg $NaPF_6$ (0.32 mmol, 2 eq.).

Yield: 57 %, red solid. ^{1}H NMR (500.10 MHz, DMSO-d6) δ = 8.49 (d, *J* = 8.8 Hz, 2H), 8.23 (d, *J* = 8.5 Hz, 1H), 8.08 (d, *J* = 8.7 Hz, 1H), 7.95 (t, *J* = 7.8 Hz, 1H), 7.74 (d, *J* = 8.8 Hz, 2H), 7.70 (t, *J* = 7.6 Hz, 1H), 7.27–7.10 (m, 16H), 6.98–6.95 (m, 4H), 5.79–5.75 (m, 2H), 5.31 (d, *J* = 2.4 Hz, 2H), 5.25–5.22 (m, 2H), 5.07 (d, *J* = 2.4 Hz, 2H), 4.64 (s, 2H) ppm. (ESI$^+$) m/z: $[M]^+$ = 847.14; calculated: 847.13; Elemental analysis calculated for $C_{51}H_{38}O_2SClMoPF_6$: C: 61.79 %, H: 3.86 %, S: 3.23 %; found: C: 62.18 %, H: 3.91 %, S: 3.31 %;

Compound 6: *Bis[η^5-1-(diphenylmethyl)cyclopentadienyl] [3-(oxo-κO)-2methyl-4H-pyran(4-thiooato-κS)] molybdenum(IV) hexafluorophosphate.* The synthesis was carried out according to the general procedure using 27 mg thiomaltol (0.19 mmol, 1.2 eq.), 13 mg NaOMe (0.24 mmol, 1.4 eq.), 100 mg **1** (0.16 mmol, 1 eq.) and 54 mg $NaPF_6$ (0.32 mmol, 2 eq.).

Yield: 65 %, brown solid. ^{1}H NMR (500.10 MHz, DMSO-d6) δ = 8.37 (d, *J* = 4.7 Hz, 1H), 7.65 (d, *J* = 4.7 Hz, 1H), 7.29–7.14 (m, 20H), 5.78 (dd, *J* = 4.7, 2.9 Hz, 2H), 5.01 (dd, *J* = 5.5, 2.8 Hz, 2H), 4.98 (dd, *J* = 4.9, 2.5 Hz, 2H), 4.82 (dd, *J* = 4.2, 2.1 Hz, 2H), 4.54 (s, 2H), 2.85 (s, 3H) ppm. (ESI$^+$) m/z: $[M]^+$ = 701.20; calculated: 701.14; Elemental analysis calculated for $C_{42}H_{35}O_2SMoPF_6$: C: 59.72 %, H: 4.18 %, S: 3.80 %; found: C: 59.77 %, H: 4.23 %, S: 3.89 %;

CCDC Deposition Numbers 2125870 (for **1**), 2125871 (for **2**), 2125872 (for **3**), 2125873 (for **4**), 2125874 (for **5**), 2125874 (for **6**) contain the supplementary crystallographic data for this paper. These data are provided free of charge by the joint Cambridge Crystallographic Data Centre and Fachinformationszentrum Karlsruhe Access Structures service.

Acknowledgements

We thank the University of Vienna and the Medical University of Vienna for financial support.

Conflict of Interest

The authors declare no conflict of interest.

Data Availability Statement

The data that support the findings of this study are available in the supplementary material of this article.

Keywords: anticancer · biological tests (in vitro and in vivo) · bioorganometallic chemistry · molybdenocenes · proteomics

[1] H. Köpf, P. Köpf-Maier, *Angew. Chem. Int. Ed. Engl.* **1979**, *18*, 477–478.
[2] P. Köpf-Maier, M. Leitner, R. Voigtländer, H. Köpf, *Z. Naturforsch. C* **1979**, *34*, 1174–1176.
[3] P. Köpf-Maier, H. Köpf, *Z., Naturforsch. B* **1979**, *34*, 805–807.
[4] P. Köpf-Maier, M. Leitner, H. Köpf, *J. Inorg. Nucl. Chem.* **1980**, *42*, 1789–1791.
[5] A. Korfel, M. E. Scheulen, H. J. Schmoll, O. Gründel, A. Harstrick, M. Knoche, L. M. Fels, M. Skorzec, F. Bach, J. Baumgart, G. Sass, S. Seeber, E. Thiel, W. E. Berdel, *Clin. Cancer Res.* **1998**, *4*, 2701–2708.
[6] C. V. Christodoulou, D. R. Ferry, D. W. Fyfe, A. Young, J. Doran, T. M. Sheehan, A. Eliopoulos, K. Hale, J. Baumgart, G. Sass, D. J. Kerr, *J. Clin. Oncol.* **1998**, *16*, 2761–2769.
[7] N. Kröger, U. R. Kleeberg, K. Mross, L. Edler, D. K. Hossfeld, *Oncol. Res.* **2000**, *23*, 60–62.
[8] G. Lümmen, H. Sperling, H. Luboldt, T. Otto, H. Rübben, *Cancer Chemother. Pharmacol.* **1998**, *42*, 415–417.
[9] I. Fichtner, D. Behrens, J. Claffey, A. Deally, B. Gleeson, S. Patil, H. Weber, M. Tacke, *Lett. Drug Des. Discovery* **2011**, *8*, 302–307.
[10] J. B. Waern, M. M. Harding, *J. Organomet. Chem.* **2004**, *689*, 4655–4668.
[11] J. L. Vera, F. R. Román, E. Meléndez, *Bioorg. Med. Chem.* **2006**, *14*, 8683–8691.
[12] J. B. Waern, M. M. Harding, *Inorg. Chem.* **2004**, *43*, 206–213.
[13] J. B. Waern, C. T. Dillon, M. M. Harding, *J. Med. Chem.* **2005**, *48*, 2093–2099.
[14] L. Y. Kuo, A. H. Liu, T.-J. Marks, *Metal Ions in Biological Systems Volume 33*, CRC Press, Boca Raton, **1996**, 53–85.
[15] G. Mokdsi, M. M. Harding, *J. Inorg. Biochem.* **2001**, *83*, 205–209.
[16] I. Feliciano, J. Matta, E. Meléndez, *J. Biol. Inorg. Chem.* **2009**, *14*, 1109–1117.
[17] D. Acevedo-Acevedo, J. Matta, E. Meléndez, *J. Organomet. Chem.* **2011**, *696*, 1032–1037.
[18] W. Kandioller, M. Reikersdorfer, S. Theiner, A. Roller, M. Hejl, M. Jakupec, M. S. Malarek, B. K. Keppler, *Organometallics* **2018**, *37*, 3909–3916.
[19] W. Kandioller, A. Kurzwenhart, M. Hanif, S. M. Meier, H. Henke, B. K. Keppler, C. Hartinger, *J. Organomet. Chem.* **2011**, *696*, 999–1010.
[20] C. M. Hackl, M. Legina, V. Pichler, M. Schmidlehner, A. Roller, O. Dömötör, E. A. Enyedy, M. Jakupec, W. Kandioller, B. K. Keppler, *Chem. Eur. J.* **2016**, *22*, 17269–17281.
[21] C. E. Pereyra, R. F. Dantas, S. B. Ferreira, L. P. Gomes, F. P. Silva-Jr, *Cancer Cell Int.* **2019**, *19*, 1–20.
[22] S. W. C. Leuthauser, L. W. Oberley, T. D. Oberley, *J. Natl. Cancer Inst.* **1982**, *68*, 123–126.
[23] R. J. Nijveldt, E. Van Nood, D. E. Van Hoorn, P. G. Boelens, K. Van Norren, P. A. Van Leeuwen, *Am. J. Clin. Nutr.* **2001**, *74*, 418–425.
[24] B. Gleeson, J. Claffey, A. Deally, M. Hogan, L. M. Méndez, H. Müller-Bunz, S. Patil, M. Tacke, *Inorg. Chim. Acta* **2010**, *363*, 1831–1836.
[25] V. Bühler, *Polyvinylpyrrolidone Excipients for Pharmaceuticals: Povidone, Crospovidone and Copovidone*, Springer, Heidelberg, **2005**.
[26] F. Fischer, S. Bauer, *Chem. Unserer Zeit* **2009**, *43*, 376–383.
[27] V. V. Strelets, S. V. Kuzharenko, G. L. Soloveichuk, A. N. Protskii, A. Rusina, *Izv. Akad. Nauk SSSR Ser. Khim.* **1985**, *7*, 1484–1490.
[28] K. Cseh, H. Geisler, K. Stanojkovska, J. Westermayr, P. Brunmayr, D. Wenisch, N. Gajic, M. Hejl, M. Schaier, G. Koellensperger, M. A. Jakupec, P. Marquetand, W. Kandioller, *Pharmaceutics.* **2022**, *14*, 2466.
[29] R. Carpenter, M. F. Brady, *BAX Gene.*, StatPearls Publishing, Treasure Island, **2020**.
[30] B. J. Aubrey, G. L. Kelly, A. Janic, M. J. Herold, A. Strasser, *Cell Death Differ.* **2018**, *25*, 104–113.
[31] J. Wang, J. Yi, *Cancer Biol. Ther.* **2008**, *7*, 1875–1884.
[32] D. Kreutz, A. Bileck, K. Plessl, D. Wolrab, M. Groessl, B. K. Keppler, S. M. Meier, C. Gerner, *Chem. Eur. J.* **2017**, *23*, 1881–1890.
[33] B. Neuditschko, A. A. Legin, D. Baier, A. Schintlmeister, S. Reipert, M. Wagner, B. K. Keppler, W. Berger, S. M. Meier-Menches, C. Gerner, *Angew. Chem. Int. Ed.* **2021**, *60*, 5063–5068; *Angew. Chem.* **2021**, *133*, 5121–5126.
[34] S. M. Meier, D. Kreutz, L. Winter, M. Klose, K. Cseh, T. Weiss, A. Bileck, B. Alte, J. C. Mader, S. Jana, A. Chatterjee, A. Bhattach, M. Hejl, M. Jakupec, P. Heffeter, W. Berger, C. Hartinger, B. K. Keppler, G. Wiche, C. Gerner, *Angew. Chem. Int. Ed.* **2017**, *56*, 8267–8271; *Angew. Chem.* **2017**, *129*, 8379–8383.
[35] D. W. Huang, B. T. Sherman, R. A. Lempicki, *Nat. Protoc.* **2009**, *4*, 44–57.
[36] Z. Shao, H. Zhao, H. Zhao, *Nucleic Acids Res.* **2009**, *37*, e16.
[37] S. M. Meier-Menches, B. Neuditschko, K. Zappe, M. Schaier, M. Gerner, K. Schmetterer, G. Del Favero, R. Bonsignore, M. Cichna-Mark, G. Koellensperger, A. Casini, C. Gerner, *Chem. Eur. J.* **2020**, *26*, 15528–15537.
[38] W. Hong, P. Cai, C. Xu, D. Cao, W. Yu, Z. Zhao, M. Huang, J. Jin, *Front. Pharmacol.* **2018**, *9*, 43.
[39] N. Sharma, A. Bhushan, J. He, G. Kaushal, V. Bhardwaj, *Cancer Metab.* **2020**, *8*, 19.
[40] D. Kreutz, C. Gerner, S. M. Meier-Menches, *Metallabiology Series: Metal-based Anticancer*, RSC, Cambridge, **2019**, 246–270.
[41] P. Fronik, M. Gutmann, P. Vician, M. Stojanovic, A. Kastner, P. Heffeter, C. Pirker, B. K. Keppler, W. Berger, C. R. Kowol, *Commun. Chem.* **2022**, *5*, 1–13.
[42] L. Kathawate, S. Gejji, S. D. Yeole, P. L. Verma, V. G. Puranik, S. A. Salunke, *J. Mol. Struct.* **2015**, *1088*, 56–63.
[43] C. X. Qin, X. Chen, R. A. Hughes, S. J. Williams, O. L. Woodman, *J. Med. Chem.* **2008**, *51*, 1874–1884.
[44] S. Chaves, M. Gil, S. Canário, R. Jelic, M. J. Romão, J. Trincão, E. Herdtweck, J. Sousa, C. Diniz, P. Fresco, M. A. Santos, *Dalton Trans.* **2008**, *13*, 1773–1782.
[45] Bruker SAINT v8.38B Copyright © 2005–2019 Bruker AXS.
[46] G. M. Sheldrick, *SADABS*, **1996**, University of Göttingen, Germany.
[47] O. V. Dolomanov, L. J. Bourhis, R. J. Gildea, J. A. K. Howard, H. Puschmann, *J. Appl. Crystallogr.* **2009**, *42*, 339–341.
[48] C. B. Huebschle, G. M. Sheldrick, B. J. Dittrich, *Appl. Crystallogr.* **2011**, *44*, 1281–1284.
[49] G. M. Sheldrick, *SHELXS v 2016/4*, **2015**, University of Göttingen, Germany.
[50] A. L. Spek, *Acta Crystallogr. Sect. D* **2009**, *65*, 148–155.

Manuscript received: August 25, 2022
Accepted manuscript online: October 12, 2022
Version of record online: ■■, ■■■

RESEARCH ARTICLE

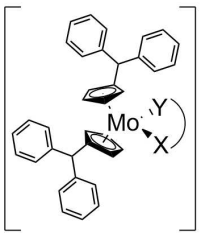

X-Y: O,O and O,S-bioactive chelate

- highest known *in vitro* cytotoxicity for Mo-complexes
- tumour growth inhibition *in vivo*
- lead compound shows strong metabolic effects in proteomic studies

A series of molybdenocenes containing lipophilic substituted Cp ligands as well as bioactive chelating ligands have shown cytotoxicity against lung, colon and ovarian cancer in vitro; one complex showed the greatest anticancer activity of any Mo-based agent known to date. Significant tumour growth inhibition was observed in in vivo studies while proteomics showed the most active compound had a strong effect on cellular metabolic processes.

V. Fuchs, K. Cseh, M. Hejl, P. Vician, B. Neuditschko, Prof. Dr. S. M. Meier-Menches, L. Janker, A. Bileck, N. Gajic, J. Kronberger, M. Schaier, S. Neumayer, Prof. Dr. G. Köllensperger, Prof. Dr. C. Gerner, Prof. Dr. W. Berger, Dr. M. A. Jakupec, M. S. Malarek, Prof. Dr. B. K. Keppler*